UNIVERSIDADE ESTADUAL DE CAMPINAS
SISTEMA DE BIBLIOTECAS DA UNICAMP
REPOSITÓRIO DA PRODUÇÃO CIENTIFICA E INTELECTUAL DA UNICAMP

Versão do arquivo anexado / Version of attached file:

Versão do Editor / Published Version

Mais informações no site da editora / Further information on publisher's website:

https://journals.aps.org/pra/abstract/10.1103/PhysRevA.95.053836

DOI: 10.1103/PhysRevA.95.053836

Direitos autorais / Publisher's copyright statement:

Oscillatory behavior of light in the composite Goos-Hänchen shift

Manoel P. Araújo[*]

Institute of Physics "Gleb Wataghin", State University of Campinas, Campinas, São Paulo, Brazil

Stefano De Leo[†]

Department of Applied Mathematics, State University of Campinas, Campinas, São Paulo, Brazil

Gabriel G. Maia[‡]

Institute of Physics "Gleb Wataghin", State University of Campinas, Campinas, São Paulo, Brazil

For incidence in the critical region, the propagation of Gaussian lasers through dielectric blocks is characterized by the joint action of angular deviations and lateral displacements. This mixed effect, known as the composite Goos-Hänchen shift, produces a lateral displacement that is dependent on the axial coordinate, recently confirmed by a weak measurement experiment. We discuss under which conditions this axial lateral displacement, which only exists for the composite Goos-Hänchen shift, presents an oscillatory behavior. This oscillation phenomenon shows a peculiar behavior of light for critical incidence and, if experimentally tested, could stimulate further theoretical studies and lead to interesting optical applications.

I. INTRODUCTION

The easiest way to describe laser propagation through dielectric structures is in terms of ray optics. The geometrical approach is useful to explain most of the practical applications [1,2]. In the extraordinary experiment realized by Goos and Hänchen in 1947 [3], the discovery of a lateral displacement of transverse-electric (TE) beams totally reflected by a dielectric-air interface suggested deviations from the laws of geometrical optics and stimulated new studies in looking for them. For $\theta_0 > \theta_{cri} + \lambda/w_0$, where θ_0 is the incidence angle at the left air-dielectric side of the triangular dielectric block depicted in Fig. 1,

$$\theta_{cri} = \arcsin[(1 - \sqrt{n^2 - 1})/\sqrt{2}] \qquad (1)$$

($\sin\theta = n \sin\psi$, $\psi = \varphi + \pi/4$, and $\sin\varphi_{cri} = 1/n$), where λ is the wavelength of the beam and w_0 its minimal waist, the Gaussian beam is totally reflected by the lower dielectric-air interface. The Fresnel coefficient is complex and acts on the whole Gaussian angular distribution. The complex phase is responsible for the transversal shift of the beam. For $\theta_0 \gg \theta_{cri} + \lambda/w_0$, the shift is of the order of λ. Its derivation, done by using the stationary phase method, appeared for the first time in the literature one year after the experiment of Goos-Hänchen and was proposed by Artmann [4]. He also observed that for transverse-magnetic (TM) beams, a different lateral displacement occurs. In 1949, this prediction was experimentally confirmed by Goos and Hänchen [5]. Approaching the critical region $\theta_0 \approx \theta_{cri} + \lambda/w_0$, the lateral displacement gains an amplification, passing from λ to $\sqrt{\lambda w_0}$ [6–8]. In the Artmann region $\theta_0 \gg \theta_{cri} + \lambda/w_0$, where the shift is proportional to λ, amplifications can be obtained by a multiple reflections device, as is the case in the first Goos-Hänchen (GH) experiment [3] or

by using the weak measurement technique [9,10], as recently done by Jayaswal *et al.* [11].

For $\theta_0 < \theta_{cri} - \lambda/w_0$, the angular Gaussian distribution is modulated by real Fresnel coefficients, the complex phase is lost, and, consequently, the lateral GH shift is not present. Nevertheless, in this incidence region, angular deviations from the laws of ray optics occur. This is due to the fact that while the incident Gaussian field,

$$I_{INC} \propto \left| \int_{-\pi/2}^{+\pi/2} d\theta\, g(\theta - \theta_0) \right.$$
$$\left. \times \exp\{ik[(\theta - \theta_0)y_{LAS} - (\theta - \theta_0)^2 z_{LAS}/2]\} \right|^2, \qquad (2)$$

has a symmetric angular distribution,

$$g(\theta - \theta_0) = \exp[-(\theta - \theta_0)^2 (kw_0)^2/4],$$

$k = 2\pi/\lambda$, centered at θ_0, and, consequently, moves along the z_{LAS} axis, the transmitted field (see Fig. 1) is

$$I_{TRA}^{[\alpha]} \propto \left| \int_{-\pi/2}^{+\pi/2} d\theta\, g(\theta - \theta_0) L_\alpha(\theta) D_\alpha(\theta) R_\alpha(\theta) \right.$$
$$\left. \times \exp\{ik[(\theta - \theta_0)(y - y_0) - (\theta - \theta_0)^2 z/2]\} \right|^2, \qquad (3)$$

where $y_0 = (\sin\theta_0 + \cos\theta_0)a + \{[\cos\theta_0 - n\cos\psi(\theta_0)]\sin\theta_0/n\cos\psi(\theta_0)\}b$ is the geometrical shift [12], α is the polarization,

$$\{L_{TE}(\theta)R_{TE}(\theta), L_{TM}(\theta)R_{TM}(\theta)\}$$
$$= \left\{ \frac{4n\cos\theta\cos\psi}{[\cos\theta + n\cos\psi]^2}, \frac{4n\cos\theta\cos\psi}{[n\cos\theta + \cos\psi]^2} \right\},$$

---
[*]mparaujo@ifi.unicamp.br
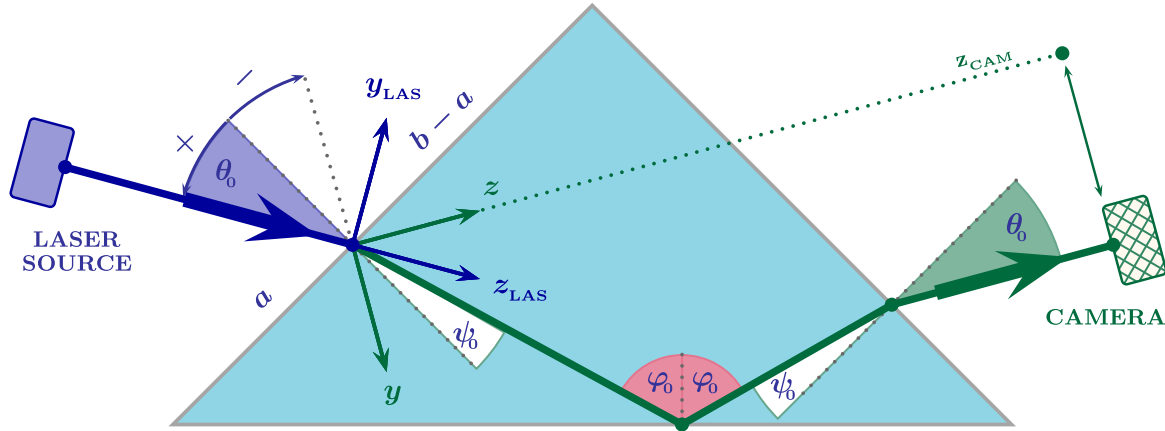[†]deleo@ime.unicamp.br
[‡]ggm11@ifi.unicamp.br

FIG. 1. The geometrical setup of the experiment on detecting oscillations. The incoming Gaussian beam propagates along the z_{INC} axis, forming an angle θ_0 (the incidence angle) with the normal to the left (air-dielectric) prism interface. Its minimal beam waist is found at the point in which the beam is refracted by the left interface. After the first refraction (ψ_0), the beam is reflected (φ_0) by the down (dielectric-air) interface and, finally, refracted (θ_0) by the right one, reaching the camera positioned at an axial distance z_{CAM} from the point of minimal beam waist.

$\sin \theta = n \sin \psi$, are the transmission Fresnel coefficients at the left and right interfaces, and

$$\{D_{\text{TE}}(\theta), D_{\text{TM}}(\theta)\}$$

$$= \left\{ \frac{n \cos \varphi - \sqrt{1 - n^2 \sin^2 \varphi}}{n \cos \varphi + \sqrt{1 - n^2 \sin^2 \varphi}}, \frac{\cos \varphi - n\sqrt{1 - n^2 \sin^2 \varphi}}{\cos \varphi + n\sqrt{1 - n^2 \sin^2 \varphi}} \right\},$$

$$(4)$$

$\varphi = \pi/4 + \psi$, the reflection coefficient at the down interface, is characterized by an angular distribution whose initial Gaussian shape is now *distorted* by the Fresnel coefficients. The symmetry breaking caused by the Fresnel coefficient [13,14] creates an axial dependence of the transversal component of the transmitted field and, as a consequence, angular deviations from the optical path predicted by the laws of geometrical optics. These deviations are of the order of $(\lambda/\text{w}_0)^2$. For transverse magnetic waves and incidence in the vicinity of the Brewster angle, the angular deviations gain an amplification of w_0/λ, leading to the giant GH angular shift [15]. This amplification has recently been detected in direct [16] and weak measurement technique-based [17,18] experiments.

The GH lateral displacement has also recently been investigated in the reflection of a light beam by a graphene layer and controlled by a voltage modulation [19] and in the reflection of terahertz radiation from a uniaxial antiferromagnetic crystal, where the action of an external magnetic field induces a nonreciprocity in the shift for positive and negative incidence [20].

We did not aim to give a complete review of theoretical analyses or experimental facts. We confined ourselves to outline the general field in which their investigation is seated. For the reader who wishes to deepen any question of lateral displacements, angular deviations, and/or breaking of symmetry in its entirety, we suggest reading the excellent works of Bliokh and Aiello [21] and Götte *et al.* [22], where clear presentations, detailed discussions, and relevant aspects of deviations from the laws of ray optics are reported.

In the next section, we give a brief discussion of the motivations which stimulated our investigation in the critical region of incidence,

$$\theta_{\text{cri}} - \lambda/\text{w}_0 < \theta_0 < \theta_{\text{cri}} + \lambda/\text{w}_0, \qquad (5)$$

where angular deviations and lateral displacements act together, generating the composite GH shift. This discussion will then be followed (Sec. III) by an analytical description of the beam transmitted through a triangular dielectric block and by the calculation of the transversal displacement of the transmitted beam as a function of its axial coordinate z. The analytical approximation is then tested and confirmed, in Sec. IV, by the numerical calculation done directly using Eq. (3). The surprising result of oscillations in the lateral displacement is, probably, the most important evidence of the strange behavior of light near the critical incidence. The conclusion and outlooks are drawn in the final section.

II. THE COMPOSITE GOOS-HÄNCHEN SHIFT

The critical region [see Eq. (5)] surely represents the most interesting incidence region to study deviations from the laws of ray optics. This is due to the fact that in this region, angular deviations and lateral displacements are both present. Furthermore, at critical incidence, the breaking of symmetry is maximized [13,14] and the Goos-Hänchen shift is amplified by a factor $\sqrt{k}\,\text{w}_0$ [6–8]. In such a region, we thus expect amplified angular deviations. Numerical calculations, done in this region, show a clear amplified axial dependence of the GH shift [23]. These (numerical theoretical) predictions have recently been confirmed by a weak measurement experimental analysis [24]. Once the amplified axial dependence is confirmed, it would be important to understand if, and if so, under which conditions negative lateral displacements occur. The idea of light oscillations around the path predicted by the geometrical optics, for incidence in the critical region, was stimulated by the fact that in this region the Gaussian angular distribution is modulated by a reflection Fresnel coefficient which is in part real ($\theta < \theta_{\text{cri}}$) and in part complex ($\theta > \theta_{\text{cri}}$). The modulated
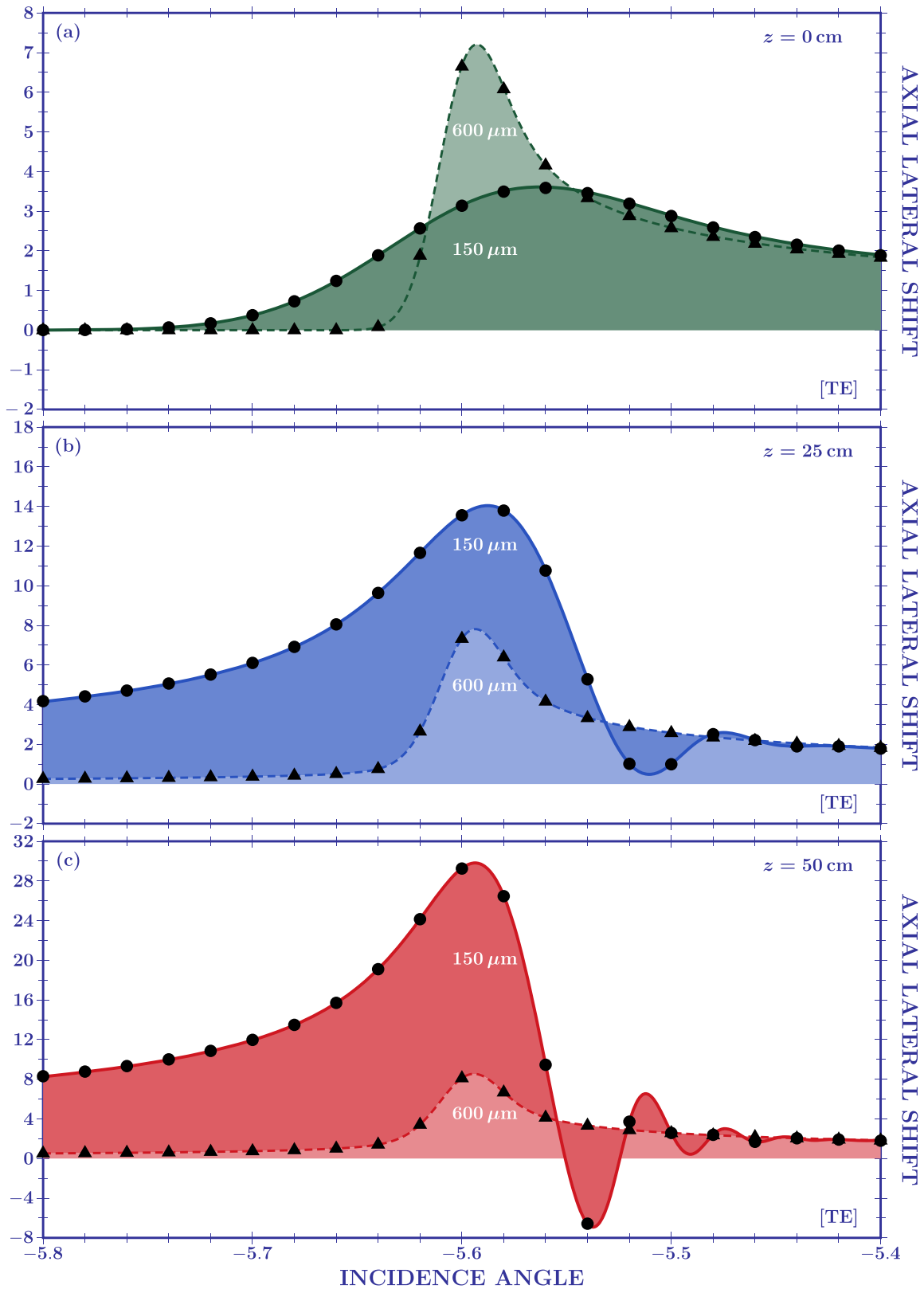
FIG. 2. Lateral displacement, as a function of the incidence angle, for TE waves. Dashed lines represent the analytical results for beams with a $w_0 = 600\,\mu$m, while solid lines are used for beams with $w_0 = 150\,\mu$m. The black circles ($150\,\mu$m) and black triangles ($600\,\mu$m) indicate the numerical data showing an excellent agreement with the analytical results. In (a), the camera is positioned very close to the right face of the prism, in (b) at $z = 25$ cm, and in (c) at $z = 50$ cm. In (a), the results of the literature are recovered. Nevertheless, as the camera moves away from the prism, an axial dependence appears, favoring beams with wider angular distributions. As z increases, we can also see oscillation phenomena.

angular distribution, which is responsible for the spatial shape of the transmitted field (no longer a Gaussian field), should present an interference between the real and complex part generating oscillation phenomena.

The possibility to find an analytical expression for the transmitted field allows one to calculate the maximal transmitted intensity and to determine the beam parameters for which oscillations can be experimentally detected. Clearly, once the analytical approximation is obtained, the analytical expression has to be tested by numerical calculations directly using the transmitted intensity given in Eq. (3). Numerical calculations are often difficult, require time, and leave obscure how to optimize the choice of the beam parameters or the experimental device. So, the analytical expression proposed in the next section could be very useful for experimentalists interested to study, investigate, and, possibly, detect, in the critical region, angular deviations from the law of geometrical optics and oscillation phenomena.

Analytical expressions for the GH shift, extensively studied in the literature, always represented an intriguing challenge. The first attempt was carried out by Artmann in 1948 [4]. Its derivation explained the lateral displacement of TE waves found in the experiment realized by Goos and Hänchen one year before [3] and predicted a different behavior of TM waves, later confirmed by Goos and Hänchen in the experiment of 1949 [5]. Nevertheless, the Artmann formula contains a divergence at the critical angle and this is due to the fact that the Taylor expansion used for the complex phase breaks down when the incidence angle approaches the critical one. In 1971 [6], Horowitz and Tamir (HT) proposed an analytical expression for the lateral displacement of a Gaussian light beam incident from a denser to a rarer medium. They obtained an approximation for the Fresnel coefficient which allowed one to analytically solve the integral determining the propagation of the reflected beam and found, for the TE and TM lateral displacements, a closed expression in terms of parabolic-cylinder (Weber) functions. They also found normalized curves that are valid for a wide range of parameters and suggested that the general functional behavior of the lateral shift should be similar for other symmetric angular distributions. In 1986 [25], Lai, Cheng, and Tang (LCT) overcame the cusplike structure in the HT formula, obtaining a theoretical result for the lateral shift of a Gaussian light beam which varies continuously and smoothly around the critical angle. Recently [8], a closed-form expression for the GH lateral displacement was proposed by Araújo, De Leo, and Maia (ADM). The ADM formula, differently from the HT and LCT ones, is not based on the reflection coefficient expansion but on the integral analysis of the complex phase. In Ref. [8], the analytical expression obtained for the lateral displacement of a Gaussian light beam neglecting the axial dependence is given in terms of modified Bessel functions of the first kind. The analysis done in [8] is also extended to different angular distribution shapes and also distinguishes between the lateral displacement of the optical beam maximum and the mean valued calculation of its shift which, due to the angular breaking of symmetry in the critical region, are different. The HT [6], LCT [25], and ADM [8] formulas reproduce, for $\theta_0 \gtrsim \theta_{cri} + \lambda/w_0$, the Artmann prediction and overcome, for incidence at critical

angle, the infinity problem. Such formulas are obtained for $z \ll z_R (= \pi w_0^2/\lambda)$ and do not contain any axial dependence. This means, for example, that to experimentally reproduce the theoretical results given in Refs. [6,8,25], the camera has to be moved very close to the (right) interface of the triangular dielectric block. Axial dependence requires a more complicated study and, often, numerical calculations [23]. Its effect, which also appears before the critical region leading to angular deviations, produces, in the critical region, an axial amplification of the lateral displacement with respect to the amplification proportional to $\sqrt{k}\, w_0$ predicted by the HT, LCT, and ADM formulas. This amplification has recently been seen in the weak measurement experiment cited in Ref. [24]. In the next section, we will find an analytical expression of the transmitted intensity without any axial simplification. So, our final formula will explicitly contain the z dependence of the camera position coming from the z-dependent term of the spatial phase appearing in Eq. (3), i.e.,

$$ k(\theta - \theta_0)^2 z/2 = [k w_0(\theta - \theta_0)]^2 z/z_R. $$

If a Gaussian beam, incident upon a dielectric-air interface (like the lower interface of the triangular prism), has its incidence angle in the critical region and if its angular distribution is broad enough ($w_0 \ll 1$ mm), plane waves in the angular spectrum with $\theta > \theta_{cri}$ will be totally internally reflected and plane waves with $\theta < \theta_{cri}$ will be partially reflected. The angular breaking of symmetry and the real ($\theta < \theta_{cri}$) and complex ($\theta > \theta_{cri}$) nature of the reflection coefficient for incidence in the critical region play a fundamental role in the oscillatory behavior of the lateral displacement seen in the composite GH shift. It is the interplay between the Goos-Hänchen shift (total internal reflection) and the angular deviations (partial reflection) which generates the composite Goos-Hänchen effect. The z dependence of the lateral displacement in the critical region [23] has recently been experimentally confirmed by using the weak measurement technique in Ref. [24]. In this paper, we analyze under which conditions an oscillatory behavior occurs and when the pattern of oscillation can be reproduced by wider beams.

The analysis presented in this paper applies to coherent light fields and leads to an analytical formula in terms of confluent hypergeometric functions of the first kind. Partially coherent light fields have to be treated by using the Mercer expansion, as done in Ref. [26].

III. TRANSMITTED INTENSITY'S ANALYTICAL EXPRESSION

To obtain an analytical formula for the transmitted beam, some approximations have to be made. The first approximation is to factorize the left-right transmission coefficients. Such coefficients are very smooth varying functions in the critical region and can thus be calculated in θ_0. The second approximation is to change the limits of integration from $\pm \pi/2$ to $\pm \infty$. This is possible as our incident Gaussian is strongly centered in θ_0, which varies between $\theta_{cri} - \lambda/w_0$ and $\theta_{cri} + \lambda/w_0$ (for BK7 prism, $\theta_{cri} = -5.603°$). Without loss of generality, we
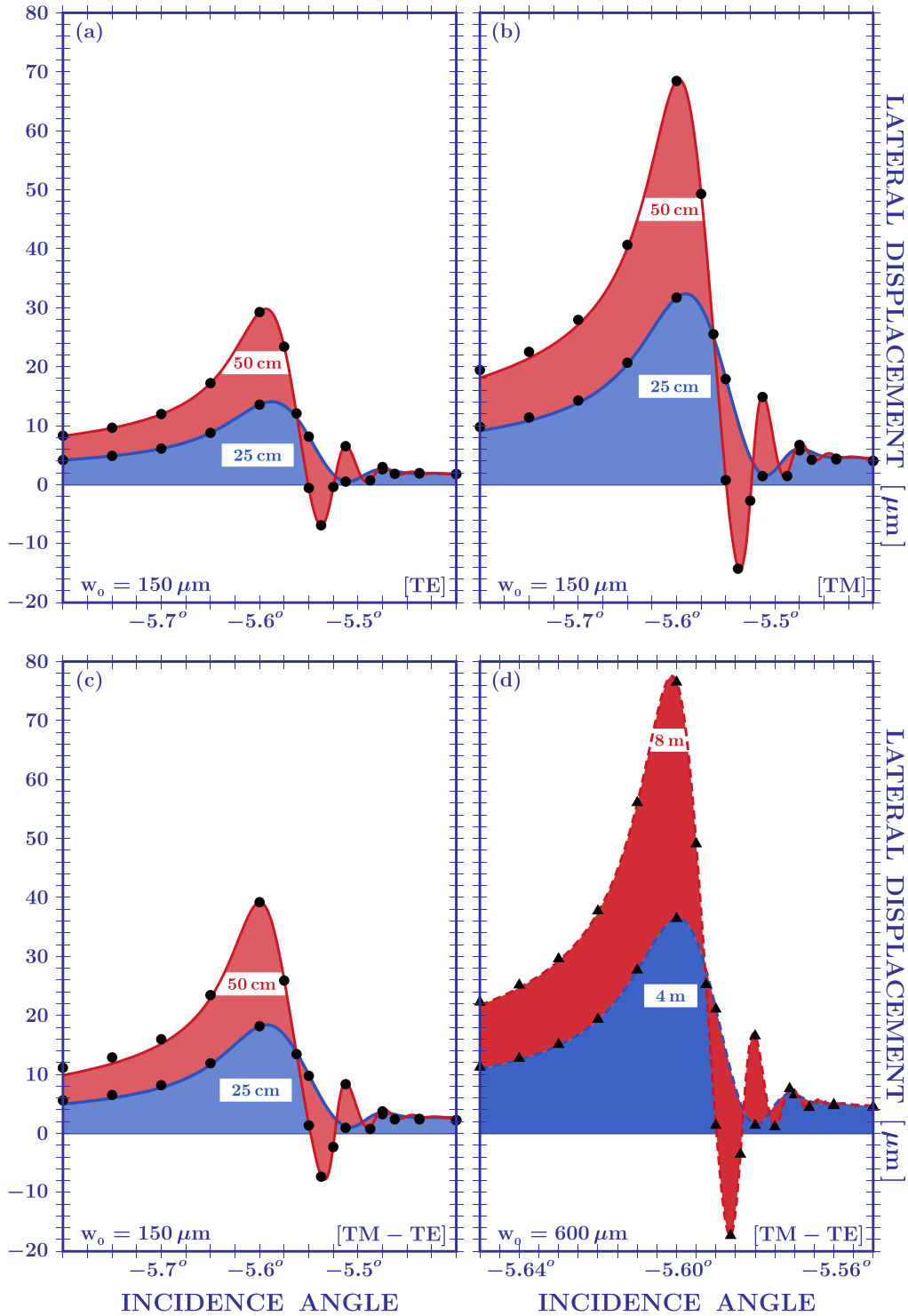
FIG. 3. (a),(b) The lateral displacement for an optical beam with $w_0 = 150 \, \mu$m is shown for TE and TM waves, respectively. For a BK7 prism, the amplification factor is 2.3. (c),(d) The lateral displacement is plotted for two different beam waists, 150 and 600 μm. For an axial distance amplified by $(w_{600}/w_{150})^2$ and an incidence region reduced by w_{150}/w_{600}, we recover in (d) the same oscillation pattern of (c). The numerical calculations (circles and triangles) show an excellent agreement with the analytical results (continuous and dashed lines). As expected, the axial dependence breaks down when the incidence angle approaches the Artmann zone where the stationary method works fine.

can thus rewrite the transmitted intensity as follows:

$$I_{\text{TRA}}^{[\alpha]} \propto \left| \int_{-\infty}^{+\infty} d\theta \, D_\alpha(\theta) \exp \left\{ -\left[\frac{k \, w_0}{2} (\theta - \theta_0) \zeta(z) \right]^2 + i k w_0 (\theta - \theta_0) \delta_{\text{GH}} \right\} \right|^2, \tag{6}$$

where $\delta_{\text{GH}} = (y - y_0)/w_0$ and $\zeta(z) = \sqrt{1 + 2iz/kw_0^2}$. The crucial point in the analytical approximation is to develop the reflection coefficient $D_\alpha(\theta)$ in square-root powers around the critical angle. To do it, we rewrite the incidence angle θ in terms of the critical one θ_{cri},

$$\theta = \theta - \theta_{\text{cri}} + \theta_{\text{cri}} = \delta\theta + \theta_{\text{cri}}.$$

By observing that

$$\sin\theta = n\sin\psi \Rightarrow \delta\theta\cos\theta_{\text{cri}} = n\,\delta\psi\cos\psi_{\text{cri}} \text{ and}$$

$$\psi = \varphi + \pi/4 \Rightarrow \delta\psi = \delta\varphi,$$

we obtain

$$\delta\varphi = \frac{\cos\theta_{\text{cri}}}{\cos\psi_{\text{cri}}}\frac{\delta\theta}{n} \approx \frac{\delta\theta}{n},$$

for BK7 $\varphi_{\text{cri}} = \arcsin(1/n) = 41.305°$, $\psi_{\text{cri}} = -3.695°$, and $\theta_{\text{cri}} = -5.603°$. By expanding around the critical angle

$$n\cos\varphi \approx n\cos\varphi_{\text{cri}} - n\sin\varphi_{\text{cri}}\delta\varphi = n\cos\varphi_{\text{cri}} - \delta\varphi,$$

$$\sqrt{1 - n^2\sin^2\varphi} \approx \sqrt{1 - n^2\sin^2\varphi_{\text{cri}} - 2n^2\sin\varphi_{\text{cri}}\cos\varphi_{\text{cri}}\delta\varphi}$$

$$= \sqrt{-2n\cos\varphi_{\text{cri}}\delta\varphi},$$

and introducing the quantity $\delta\phi = -\delta\varphi/n\cos\psi_{\text{cri}}$, we can approximate the TE and TM reflection coefficients, given in (4), as follows:

$$D_{\text{TE}} = \frac{1 + \delta\phi - \sqrt{2\,\delta\phi}}{1 + \delta\phi + \sqrt{2\,\delta\phi}} \approx 1 - 2\sqrt{2\delta\phi} - 4\delta\phi,$$

$$D_{\text{TM}} = \frac{1 + \delta\phi - n^2\sqrt{2\,\delta\phi}}{1 + \delta\phi + n^2\sqrt{2\delta\phi}} \approx 1 - 2n^2\sqrt{2\,\delta\phi} - 4n^2\delta\phi.$$

Finally,

$$D_\alpha(\theta) \approx 1 - \sqrt{2\gamma_\alpha(\theta_{\text{cri}} - \theta)} + \gamma_\alpha(\theta_{\text{cri}} - \theta), \quad (7)$$

where $\{\gamma_{\text{TE}}, \gamma_{\text{TM}}\} = 4\{1, n^4\}/n\sqrt{n^2 - 1}$. By using this expansion and introducing the new integration variable $\tau = kw_0\zeta(z)(\theta_{\text{cri}} - \theta)/2$, we obtain

$$I_{\text{TRA}}^{[\alpha]} \propto \left|\int_{-\infty}^{+\infty} d\tau\left[1 - 2\sqrt{\frac{\gamma_\alpha\tau}{kw_0\zeta(z)}} + \frac{2\gamma_\alpha\tau}{kw_0\zeta(z)}\right]\right.$$

$$\left.\times \exp\{-[\tau + d(\delta_{\text{GH}}, z)]^2\}\right|^2 \mathcal{G}(\delta_{\text{GH}}, z), \quad (8)$$

where

$$d(\delta_{\text{GH}}, z; \theta_0) = k\,w_0\,\zeta(z)(\theta_0 - \theta_{\text{cri}})/2 + i\,\delta_{\text{GH}}/\zeta(z)$$

contains, besides the transversal and axial variables, the incidence angle dependence and $\mathcal{G}(\delta_{\text{GH}}, z)$ represents the Gaussian function $\exp[-2\delta_{\text{GH}}^2/|\zeta(z)|^4]$. The square-root and linear terms in the brackets of Eq. (8) act as modulators of the Gaussian function $\mathcal{G}(\delta_{\text{GH}}, z)$. The effect of their modulation can be evaluated once the integral in Eq. (8) is analytically solved.

To do this, we observe that the integral with a square-root integrand can be converted into a series,

$$\int_{-\infty}^{+\infty} d\tau\sqrt{\tau}\exp[-(\tau + d)^2]$$

$$= \exp[-d^2]\sum_{m=0}^{\infty}\frac{(-2d)^m}{m!}\int_{-\infty}^{+\infty}d\tau\,\tau^{m+\frac{1}{2}}\exp[-\tau^2]$$

$$= \exp[-d^2]\sum_{m=0}^{\infty}\frac{(2d)^m}{m!}\frac{(-1)^m + 1}{2}\Gamma\left(\frac{2m + 3}{4}\right). \quad (9)$$

The series that is found is a well-known Gamma functions series leading to a combination of confluent hypergeometric functions of the first kind. Thus, the integral can be analytically solved in terms of these functions,

$$\int_{-\infty}^{+\infty} d\tau\sqrt{\tau}\exp[-(\tau + d)^2] = \frac{e^{i\frac{\pi}{4}}}{2\sqrt{2}}\mathcal{F}(\delta_{\text{GH}}, z; \theta_0), \quad (10)$$

where

$$\mathcal{F}(\delta_{\text{GH}}, z; \theta_0)$$
$$= \left[2\Gamma\left(\tfrac{3}{4}\right){}_1F_1\left(\tfrac{3}{4}, \tfrac{1}{2}, d^2\right) + i\Gamma\left(\tfrac{1}{4}\right){}_1F_1\left(\tfrac{5}{4}, \tfrac{3}{2}, d^2\right)d\right]\exp[-d^2].$$

Finally, the analytical approximation for the transmitted intensity is given by

$$I_{\text{TRA}}^{[\alpha]} \propto \left|1 - \sqrt{\frac{\gamma_\alpha}{2\pi kw_0\zeta(z)}}e^{i\frac{\pi}{4}}\mathcal{F}(\delta_{\text{GH}}, z; \theta_0)\right.$$

$$\left. - \frac{2\gamma_\alpha d(\delta_{\text{GH}}, z; \theta_0)}{kw_0\zeta(z)}\right|^2 \mathcal{G}(\delta_{\text{GH}}, z). \quad (11)$$

The study of the maximum of this function will be the topic of the next section.

IV. THE AXIAL OSCILLATORY BEHAVIOR

In order to check the validity of our approximation and compare our results with the previous ones that have appeared in the literature, we first analyze the case in which the axial dependence is removed from Eq. (11). In the experimental setup, this means the case in which the camera is positioned very close to the right side of the dielectric block, i.e., $z \ll z_R$. This is, for example, the situation of the experiment done by Cowan and Anicin in Ref. [27]. In such an experiment, the collected data were compared with the theoretical formulas of Artmann [4] and Tamir and Horowitz [6]. In Fig. 2(a), we plot, for TE waves, the lateral displacement for a laser Gaussian beam with wavelength $\lambda = 0.633$ (the wavelength of choice for most HeNe lasers) and beam waists of 150, 300, and 600 μm transmitted through a triangular BK7 ($n = 1.515$) block and detected by a camera very close to the right side of the dielectric block. As observed, this means removing the axial dependence in Eq. (11). In this case, we obtain, in accordance with the previous theoretical calculations that have appeared in the literature [6,8,25], an amplification of the lateral shift proportional to $\sqrt{kw_0}$ for critical incidence; see Fig. 2(a). In this approximation, the amplification prefers wider spatial distributions. The numerical calculations, obtained by directly using Eq. (6) with $\zeta(z) \approx 1$, are in excellent agreement
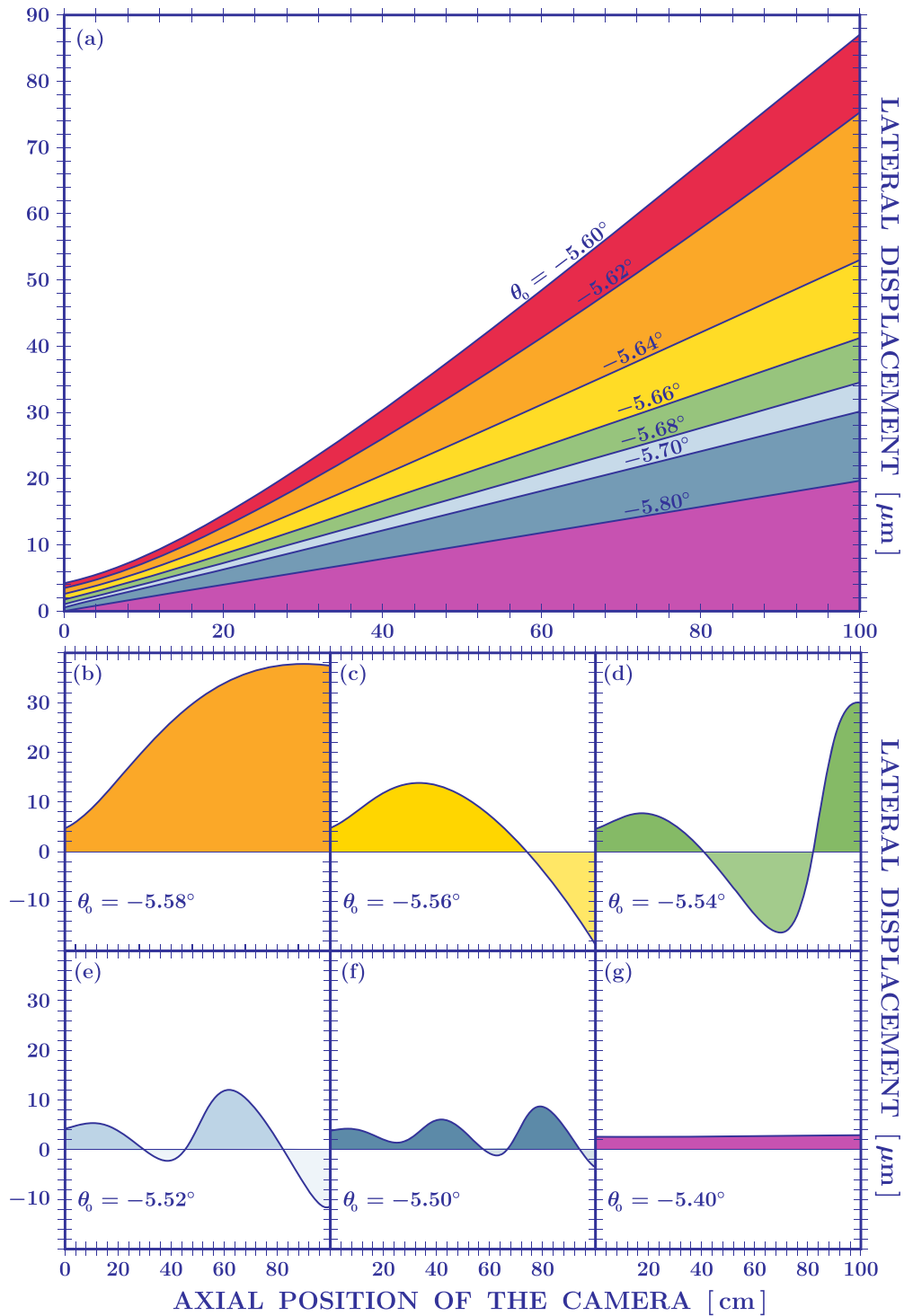
FIG. 4. Lateral displacement as a function of the axial position of the camera. In (a), the phenomenon of angular deviations as well as its amplification for incidence angles approaching the critical one is evident. In (b)–(f), oscillations are visible. Their amplitude is reduced when the incidence angle approaches the left border of the critical region. In (g), the symmetry of the angular distribution is completely recovered and angular deviations as well as oscillations are lost.

with the results predicted by the analytical formula given by Eq. (11) for $z \approx 0$. Phenomena as angular deviations and/or oscillations cannot be seen in this case. By moving the camera away from the right side of the dielectric block, along the axial propagation direction of the transmitted beam predicted by geometric optics, an additional z-dependent

lateral displacement appears. This is, for example, the case of the experimental setup in Ref. [28]. This z-dependent lateral displacement is called, in the literature, angular shift. This angular shift is clearly visible in the left incidence region of Figs. 2(b) and 2(c). The axial dependence for the critical region mixes two effects: the angular deviations (caused

by the symmetry breaking of the angular distribution) and the GH shift (caused by the additional complex phase in the Fresnel coefficient). This mixed effect, known as composite GH shift, was recently proven by a weak measurement experiment [24]. The axial effects depend on the ratio z/z_R and, consequently, for a fixed axial position of the camera, narrower spatial beams experience larger amplifications. This can be understood by observing that narrower spatial beams have wider angular distributions and, consequently, they are more sensible to the breaking of symmetry caused by the Fresnel reflection coefficient. This axial amplification, different from the standard amplification obtained for $z \approx 0$, is clearly seen in the plots of Figs. 2(b) and 2(c). In such plots, we also see oscillation phenomena for $w_0 = 150\ \mu$m. The numerical data show an excellent agreement with the analytical calculation. The axial amplification was recently confirmed by the experiment done in Ref. [24]. Nevertheless, the oscillatory behavior was not detected in such an experiment because, as seen in Figs. 2(b) and 2(c), the oscillatory behavior starts, for a beam waist of 150 μm, from an axial position of the camera of 25 cm and it is seen for incidence greater than the critical ones. In the referred experimental article, the beam waist is 170 μm, the camera positioned at $z = 20$ and 25 cm, and the incidence angle not great enough to reach the right zone of the critical region. The mathematical explanation of the oscillation phenomenon comes from the presence of confluent hypergeometric functions in the transmitted intensity. For $\theta_0 \leqslant \theta_{\mathrm{cri}}$ (the dominant part of d is the real one) and $\theta_0 \geqslant \theta_{\mathrm{cri}} + \lambda/w_0$ (the dominant part of d is the imaginary one), the argument of the confluent hypergeometric functions is real and no oscillation can be seen. In the right zone of the critical region, $\theta_{\mathrm{cri}} \leqslant \theta_0 \geqslant \theta_{\mathrm{cri}} + \lambda/w_0$, depending on the value of z/z_R, the real and complex parts of d become comparable and the confluent hypergeometric functions will have a complex argument, opening the door to oscillation phenomena. For increasing values of the incidence angle, the beam reaches the Artmann zone and the angular distribution recovers its original Gaussian symmetry leading to the Artmann results. In this incidence region, the composite GH shift tends to the standard GH shift, which only depends on the geometrical dielectric structure and on the beam wavelength, and, consequently, the shift does not depend on the beam waist; see the right zone of the critical incidence in Figs. 2.

The amplification $\sqrt{\gamma_{\mathrm{TM}}/\gamma_{\mathrm{TE}}} = n^2$ between TE and TM waves is of a factor 2.3 (BK7 prism) and it is shown in Figs. 3(a) and 3(b). The amplification between the different beam waist 150 μm [Fig. 3(c)] and 600 μm [Fig. 3(d)] is of a factor $\sqrt{w_{600}/w_{150}} = 2$. The fact that the axial coordinate z always appears in the analytical formula with the denominator kw_0^2 also allows one to predict, given two different Gaussian beam waists, when it is possible to visualize the same pattern of oscillation. For the cases examined in our study, the axial coordinate multiplication factor is given by $z_{600}/z_{150} = (w_{600}/w_{156})^2 = 16$. According to the results shown in Fig. 3, it seems that by increasing the beam waist, we improve our experimental measurement. In reality, what we improve is the lateral displacement of a factor $\sqrt{w_{600}/w_{150}} = 2$. Nevertheless, what we measure is the lateral displacement of a beam with waist $w(z)$. Thus, it would be more appropriate to introduce an adimensional quantity given by the ratio

between the lateral displacement and the beam waist at the axial point where the camera is located. This ratio assesses the experimental performance needed to measure the lateral displacement. For the cases examined in Figs. 3(c) and 3(d), we have $\sqrt{\lambda/w_{150}}$ and $\sqrt{\lambda/w_{600}}$, respectively, clearly showing a better efficiency for a measurement done with a beam waist of 150 μm.

The analysis presented in Fig. 4 has been carried out by calculating the lateral displacement as a function of the incidence angle θ_0 for different axial positions of the camera. It is also interesting to calculate such a displacement as a function of the axial position z for fixed incidence angles. Approaching the critical angle from the left [see Fig. 4(a)], we have the phenomenon of amplification of the angular deviations (caused by the angular symmetry breaking of the transmitted beam), i.e., $0.0011°$ ($\theta_0 = -5.8°$), $0.0017°$ ($-5.7°$), and $0.0055°$ ($-5.6°$). For incidence greater that the critical angle, the oscillating GH shift appears; see Figs. 4(c)–4(f). Fixing the incidence angle at $\theta_0 = -5.54°$, and varying the axial position of the camera at $z = 20, 40, 70, 100$ cm, we would find a pattern of oscillating GH displacement, $7.6, 0.4 - 16.3, 30.0\ \mu$m. The amplitude of oscillation decreases when the incidence angle approaches the right border of the critical region [29].

V. CONCLUSIONS

Finally, we can conclude that in the critical region, for $\theta_0 < \theta_{\mathrm{cri}}$, the real part of the angular distribution wins over the complex one and angular deviations are the main evidence of the angular breaking of symmetry. For $\theta_0 > \theta_{\mathrm{cri}}$, the situation is reversed and the main contribution comes from the complex part generating oscillation phenomena. By increasing the incidence angle and approaching the right border of the critical region, the real part of the angular distribution vanishes and we recover the Gaussian symmetry in the transmitted beam. In this case, we do not find any notable angular deviations. The beam practically moves along the z axis, but it is transversally displaced by the GH shift. For incidence at $\theta_0 = -5.4°$ and different axial positions of the camera, say 20, 40, 70, 100 cm, we, for example, find the following lateral displacements: 2.6, 2.7, 2.8, 2.9 μm.

To conclude this work, let us emphasize once more that the challenge of detecting deviations from the laws of geometrical optics is still a current issue of optics containing a number of unsolved and, at the same time, interesting questions of very general significance. We have not given a rigorous mathematical elaboration of the theory, but only a simplified analytical formula to calculate angular deviations and oscillation phenomena in the critical region. It is the authors hope that this study will find many readers among theoretical and experimental physicists and specialists in related branches of optics, and help them in future theoretical studies as well as stimulating experiments that could confirm the oscillatory Goos-Hänchen shift.

[1] M. Born and E. Wolf, *Principles of Optics* (Cambridge University Press, Cambridge, 1999).

[2] B. E. A. Saleh and M. C. Teich, *Fundamentals of Photonics* (Wiley, New Jersey, 2007).

[3] F. Goos and H. Hänchen, A new and fundamental experiment regarding total reflection, Ann. Phys. **436**, 333 (1947).

[4] K. Artmann, Calculation of the lateral displacement of the totally reflected beam, Ann. Phys. **437**, 87 (1948).

[5] F. Goos and H. Hänchen, New measurement of the beam displacement effect at total reflection, Ann. Phys. **440**, 251 (1949).

[6] B. R. Horowitz and T. Tamir, Lateral displacement of a light beam at a dielectric interface, J. Opt. Soc. Am. **61**, 586 (1971).

[7] M. P. Aráujo, S. A. Carvalho, and S. De Leo, The frequency crossover for the Goos-Hänchen shift, J. Mod. Opt. **60**, 1772 (2013).

[8] M. P. Aráujo, S. De Leo, and G. G. Maia, Closed-form expression for the Goos-Hanchen lateral displacement, Phys. Rev. A **93**, 023801 (2016).

[9] Y. Aharonov, D. Z. Albert, and L. Vaidman, How the result of a measurement of a component of the spin of a spin 1/2 particle can turn out to be 100, Phys. Rev. Lett. **60**, 1351 (1988).

[10] I. M. Duck, P. M. Stevenson, and E. C. G. Sudarshan, The sense in which a "weak measurement" of a spin-½ particle's spin component yields a value 100, Phys. Rev. D **40**, 2112 (1989).

[11] G. Jayaswal, G. Mistura, and M. Merano, Weak measurement of the Goos-Hänchen shift, Opt. Lett. **38**, 1232 (2013).

[12] S. Carvalho and S. De Leo, The use of the stationary phase method as a mathematical tool to determine the path of optical beams, Am. J. Phys. **83**, 249 (2015).

[13] M. P. Araujo, S. A. Carvalho, and S. De Leo, The asymmetric Goos-Hänchen effect, J. Opt. **16**, 015702 (2014).

[14] M. P. Aráujo, S. A. Carvalho, and S. De Leo, Maximal breaking of symmetry at critical angle and closed-form expression for angular deviations of the Snell law, Phys. Rev. A **90**, 033844 (2014).

[15] C. C. Chan and T. Tamir, Angular shift of a Gaussian beam reflected near the Brewster angle, Opt. Lett. **10**, 378 (1985).

[16] M. Merano, A. Aiello, M. P. van Exter, and J. P. Woerdman, Observing angular deviations in the specular reflection of a light beam, Nat. Photon. **3**, 337 (2009).

[17] S. Goswami, M. Pal, A. Nandi, P. K. Panigrahi, and N. Ghosh, Simultaneous weak value amplification of angular Goos-Hänchen and Imbert-Fedorov shifts in partial reflection, Opt. Lett. **39**, 6229 (2014).

[18] G. Jayaswal, G. Mistura, and M. Merano, Observing angular deviations in light-beam reflection via weak measurements, Opt. Lett. **39**, 6257 (2014).

[19] M. Cheng, P. Fu, X. Chen, X. Zeng, S. Feng, and R. Chen, Giant and tunable Goos-Hanchen shifts for attenuated total reflection structure containing graphene, J. Opt. Soc. Am. B **31**, 2325 (2014).

[20] R. Macêdo, R. L. Stamps, and T. Dumelow, Spin canting induced nonreciprocal Goos-Hänchen shifts, Opt. Express **22**, 28467 (2014).

[21] K. Y. Bliokh and A. Aiello, Goos-Hänchen and Imbert-Fedorov beam shifts: An overview, J. Opt. **15**, 014001 (2013).

[22] J. B. Götte, S. Shinohara, and M. Hentschel, Are Fresnel filtering and the angular Goos-Hänchen shift the same?, J. Opt. **15**, 014009 (2013).

[23] M. P. Araújo, S. De Leo and G. G. Maia, Axial dependence of optical weak measurements in the critical region, J. Opt. **17**, 035608 (2015).

[24] O. Santana, S. Carvalho, S. De Leo, and L. Araujo, Weak measurement of the composite Goos-Hänchen shift in the critical region, Opt. Lett. **41**, 3884 (2016).

[25] H. M. Lai, F. C. Cheng, and W. K. Tang, Goos-Hänchen effect around and off the critical angle, J. Opt. Soc. Am. A **3**, 550 (1986).

[26] L. G. Wang, S. Y. Zhu, and M. S. Zubairy, Goos-Hänchen shifts of partially coherent light fields, Phys. Rev. Lett. **111**, 223901 (2013).

[27] J. J. Conwan and B. Anicin, Longitudinal and transverse displacements of a bounded microwave beam at total internal reflection, J. Opt. Soc. Am. **67**, 1307 (1977).

[28] D. Müller, D. Tharanga, A. A. Stahlhofen, and G. Nimtz, Nonspecular shifts of microwaves in partial reflection, Europhys. Lett. **73**, 526 (2006).

[29] See Supplemental Material at http://link.aps.org/supplemental/10.1103/PhysRevA.95.053836 for the oscillatory behavior of the GH shift in the critical region.